




# Absence of Subcerebral Projection Neurons Is Beneficial in a Mouse Model of Amyotrophic Lateral Sclerosis

Thibaut Burg, PhD <sup>1</sup>, Charlotte Bichara, MSc,<sup>2</sup> Jelena Scekcic-Zahirovic, MD, PhD,<sup>1</sup> Mathieu Fischer, MSc <sup>1†</sup>, Geoffrey Stuart-Lopez, MSc,<sup>1</sup> Aurore Brunet, MSc,<sup>1</sup> François Lefebvre, MD, PhD,<sup>3</sup> Matilde Cordero-Erausquin, PhD,<sup>2</sup> and Caroline Rouaux, PhD <sup>1†</sup>

**Objective:** Recent studies carried out on amyotrophic lateral sclerosis patients suggest that the disease might initiate in the motor cortex and spread to its targets along the corticofugal tracts. In this study, we aimed to test the corticofugal hypothesis of amyotrophic lateral sclerosis experimentally.

**Methods:** *Sod1*<sup>G86R</sup> and *Fezf2* knockout mouse lines were crossed to generate a model that expresses a mutant of the murine *Sod1* gene ubiquitously, a condition sufficient to induce progressive motor symptoms and premature death, but genetically lacks corticospinal neurons and other subcerebral projection neurons, one of the main populations of corticofugal neurons. Disease onset and survival were recorded, and weight and motor behavior were followed longitudinally. Hyper-reflexia and spasticity were monitored using electromyographic recordings. Neurodegeneration and gliosis were assessed by histological techniques.

**Results:** Absence of subcerebral projection neurons delayed disease onset, reduced weight loss and motor impairment, and increased survival without modifying disease duration. Absence of corticospinal neurons also limited presymptomatic hyper-reflexia, a typical component of the upper motoneuron syndrome.

**Interpretation:** Major corticofugal tracts are crucial to the onset and progression of amyotrophic lateral sclerosis. In the context of the disease, subcerebral projection neurons might carry detrimental signals to their downstream targets. In its entirety, this study provides the first experimental arguments in favor of the corticofugal hypothesis of amyotrophic lateral sclerosis.

ANN NEUROL 2020;88:688–702

Amyotrophic lateral sclerosis (ALS) is a devastating neurodegenerative disease characterized by rapidly progressing muscle atrophy and paralysis, leading to death within only 2 to 5 years of diagnosis. Clinically and histologically, ALS is defined as the progressive loss of two neuronal populations: corticospinal and corticobulbar neurons (CSN) in the motor cortex, and spinal and bulbar

motoneurons (MN) in the brainstem and spinal cord.<sup>1</sup> This duality has fostered a long-standing debate regarding the disease origin along the corticospinomuscular axis.<sup>2</sup>

Jean-Martin Charcot, who first described ALS, suggested a cortical origin and a propagation from the motor cortex to the spinal cord.<sup>3</sup> Comprehensive clinical examination of patients unraveled signs highly suggestive

View this article online at [wileyonlinelibrary.com](http://wileyonlinelibrary.com). DOI: 10.1002/ana.25833

Received Dec 6, 2019, and in revised form Jun 23, 2020. Accepted for publication Jun 23, 2020.

Address correspondence to Dr Caroline Rouaux, Inserm UMR\_S 1118, Mécanismes centraux et périphériques de la neurodégénérescence, Faculté de Médecine, Université de Strasbourg, Strasbourg, France. E-mail: [caroline.rouaux@inserm.fr](mailto:caroline.rouaux@inserm.fr)

<sup>†</sup>Current address: Department of Paediatrics, John Radcliffe Hospital, University of Oxford, Oxford, UK.

From the <sup>1</sup>Inserm UMR\_S 1118, Mécanismes centraux et périphériques de la neurodégénérescence, Faculté de Médecine, Université de Strasbourg, Strasbourg, France; <sup>2</sup>UPR 3212, Institut des neurosciences cellulaires et intégratives, UPR 3212 CNRS, Université de Strasbourg, Strasbourg, France; and <sup>3</sup>GMRC, service de santé publique, Hôpitaux Universitaires de Strasbourg, Strasbourg, France

Additional supporting information can be found in the online version of this article.

of a cortical origin, such as the split hand syndrome and typical gait abnormalities.<sup>4</sup> Meanwhile, transcranial magnetic stimulation studies identified early hyperexcitability of the motor cortex that is negatively correlated with survival and manifests before disease onset, pointing again to a potentially initiating role of the motor cortex.<sup>5</sup> Cortical hyperexcitability has been proposed to translate into glutamatergic excitotoxicity to downstream targets of the CSN, ie, spinal and bulbar MN, providing a first possible mechanism for propagation.<sup>4</sup> More recently, staging of the TAR DNA binding protein (TARDBP; also known as TDP-43) pathology,<sup>6</sup> a histopathological burden that characterizes most ALS patients, led to the emergence of the so-called corticofugal hypothesis, which proposes a motor cortical origin of the disease and a direct, monosynaptic dissemination of misfolded TDP-43 proteins in a prion-like manner.<sup>7</sup> Although supported by several neuroimaging studies (reviewed by Brunet and colleagues<sup>8</sup>), corticofugal propagation cannot be assessed in patients. We thus reasoned that mouse genetics could prove useful to address a potential cortical origin and corticofugal propagation of ALS directly.

In rodents, as in humans, corticofugal projections arise from two populations: corticothalamic projection neurons and subcerebral projection neurons (SubCerPN) that include the disease-relevant CSN.<sup>9,10</sup> Although major differences exist between primates and rodents regarding the route of the corticospinal tract and the connectivity of CSN onto alpha motoneurons, many mouse models of ALS recapitulate CSN or SubCerPN degeneration (reviewed by Brunet and colleagues<sup>8</sup>). Likewise, we recently showed that *Sod1*<sup>G86R</sup> mice display presymptomatic CSN degeneration and a somatotopic relationship between CSN and spinal motoneuron degeneration,<sup>11</sup> as reported in ALS patients.<sup>12</sup>

Here, we sought to test the contribution SubCerPN to ALS by taking advantage of the *Fezf2* knockout mice that develop in the absence of SubCerPN.<sup>13</sup> These animals lack the gene encoding the transcription factor *Fezf2* (*Fezl*, *Zfp312*) that is both necessary<sup>14</sup> and sufficient to instruct birth and specification of CSN and other SubCerPN.<sup>15,16</sup> *Fezf2*<sup>-/-</sup> mice are hyperactive,<sup>13</sup> present defects of cortical interneuron lamination and unbalanced cortical activity,<sup>17</sup> and fail to feed on solid food.<sup>13</sup> However, when fed soft food, *Fezf2*<sup>-/-</sup> mice do not display any major motor phenotype: they walk and reproduce. We crossbred the *Sod1*<sup>G86R</sup> and *Fezf2*<sup>-/-</sup> mouse lines to generate a model ubiquitously expressing the *Sod1*<sup>G86R</sup> transgene, a condition sufficient to develop an ALS-like phenotype,<sup>18</sup> but entirely lacking CSN and other SubCerPN, hence challenging the definition of ALS.

An initial report of the findings presented here was published as a preprint on bioRxiv.<sup>19</sup>

## Materials and Methods

### Animals

All animal experiments were performed by authorized investigators and approved by the local ethical committee of Strasbourg University (CREMEAS, agreement #00738.01). Animals, kept 2 to 5 per cages, were housed in the animal facility of the Faculty of Medicine of Strasbourg, with a regular 12 hour/12 hour light/dark cycle, in constant conditions (21 ± 1°C; 60% relative humidity). Food and water were accessible ad libitum. *Fezf2*<sup>-/-</sup> mice<sup>13</sup> were obtained from the Arlotta Laboratory. *Sod1*<sup>G86R</sup> males<sup>18</sup> were crossed with *Fezf2*<sup>+/-</sup> females, and F1 *Fezf2*<sup>+/-</sup>/*Sod1*<sup>G86R</sup> males were crossed with *Fezf2*<sup>+/-</sup>/WT females to obtain *Fezf2*<sup>+/-</sup>/WT (WT, n = 23); *Fezf2*<sup>-/-</sup>/WT (KO, n = 22); *Fezf2*<sup>+/-</sup>/*Sod1*<sup>G86R</sup> (*Sod1*, n = 14); and *Fezf2*<sup>-/-</sup>/*Sod1*<sup>G86R</sup> (KO/*Sod1*, n = 17). Males were used for survival, behavior, and histology. Males and females, in equal proportions, were used for H-reflex (n = 6 WT, n = 6 KO, n = *Sod1*, and n = KO/*Sod1*) and histology (75 days: n = 6 WT, n = 5 KO, n = 6 *Sod1*, and n = 3 KO/*Sod1*; and 105 days: n = 6 WT, n = 4 KO, n = 8 *Sod1*, and n = 5 KO/*Sod1*).

### Quantitative PCR Analyses

Tissue harvesting, RNA extraction, and qPCR were performed as described by Scekcic-Zahirovic and colleagues<sup>20</sup> using the following primers: *Gusb*, forward, 5'-CGAGTATGGAGCAGACGCA A-3' and reverse, 5'-AGCCTTCTGGTACTCCTCACT-3'; *Actb*, forward, 5'-ATGTGGATCAGCAAGCAGGA-3' and reverse, 5'-AGCTCAGTAACAGTCCGCCT-3'; *Hsp90ab1*, forward, 5'-TACTACTCGGCTTCCCGTCA-3' and reverse, 5'-CCTGAAAGGCCAAAGGTCTCCA-3'; *Fezf2*, forward, 5'-GT GCGGCAAGGTGTTCAATG-3' and reverse, 5'-CAGACTTT GCACACAAACGGT-3'; *Sod1*, forward, 5'-GAGACCTGGGC AATGTGACT-3' and reverse, 5'-GTTTACTGCGCAATCCC AAT-3'; and *Chat*, forward, 5'-CTGGCCACCTACCTTC AGTG-3' and reverse, 5'-CCCCAAACCGCTTCACAATG-3'.

### Motor Tests and Regression Analyses

Mice were trained from 5 to 8 weeks of age and followed from 9 weeks until death. Motor coordination, endurance, muscle strength, and mouse gait were assessed as previously described.<sup>20</sup> Multiple linear regression analyses were run on R v.3.4.3 with all the relevant packages to include weight and speed as confounding variables. Normality of distributions was tested using the Shapiro–Wilk or the Kolmogorov–Smirnov test and assessed graphically using a normal quantile plot.

### Electromyography, H-Reflex, and Tail Long Lasting Reflex Recordings

All recordings were performed with a standard electromyographic apparatus (Dantec Dynamics, Skovlunde, Denmark) as previously described.<sup>21</sup> Tail spasticity of end-stage mice was determined and quantified as previously described.<sup>22</sup> Signal intensities were measured before and after stimulation, using ImageJ (US,

National Institutes of Health, Bethesda, MD). The H-reflex was assessed on presymptomatic mice aged 80 and 105 days (first and second hindlimb, respectively), by modifying a previously described method,<sup>23</sup> with stimulation of the sciatic nerve and recording in the abductor digiti minimi muscles. The amplitude of the H-reflex, as the peak–trough value of the recording on a 1 millisecond window situated at the expected latency for the H-reflex, was measured between 5 and 8 milliseconds after stimulation. Mice were considered to display an H-reflex when at least 1 of the 2 hindlimbs was positive.

### Retrograde Labeling of the CSN and Histological Procedures

CSN were retrogradely labeled with Fluorogold as previously described.<sup>14</sup> Animals were transcardially perfused with 4% paraformaldehyde (PFA) as described.<sup>20</sup> Nervous tissues were cut into 40- $\mu$ m-thick vibratome sections (Leica Biosystems, Wetzlar, Germany). Sections were blocked for 30 minutes with 5% horse serum and 0.5% Triton X-100, incubated with primary antibody overnight, rinsed in phosphate-buffered saline and incubated for 2 hours with secondary antibody (1/500, Jackson Immuno-research, West Grove, PA).

For immunohistochemistry, sections were pretreated for 10 minutes in 3% H<sub>2</sub>O<sub>2</sub> and revealed upon 1 hour incubation in Vectastain ABC Kit (Vector Laboratories, Burlingame, CA) with 0.075% 3,3'-diaminobenzidine (Sigma-Aldrich, St Louis, MO) and 0.002% H<sub>2</sub>O<sub>2</sub> in 50mM Tris–HCl. Primary antibodies were as follows: goat anti-ChAT (AB144P, 1/50), mouse anti-parvalbumin (MAB1572,1/500), and goat anti-calretinin (AB1550,1/1000) (Millipore, Burlington, MA); rat anti-CTIP2 (AB18465, 1/100), mouse anti-P62 (AB56416, 1/100), goat anti-TPH2 (AB121013, 1/500), and goat anti-Iba1 (AB5076, 1/100) (Abcam, Cambridge, UK); rabbit anti-synaptophysin (578, 1/100) and rabbit anti-neurofilament (NF575, 1/100) (Eurogentec, Seraing, Belgium); mouse anti-CRYM (AA215-314,1/100, Abnova, Taipei, Taiwan); rabbit anti-GFAP (Z0334, 1/200, Dako, Agilent, Santa Clara, CA); rat anti-TDP-43 (10782-2-AP,1/500, Proteintech, Rosemont, IL); and mouse anti-calbindin (C9848,1/500) and rhodamine-conjugated  $\alpha$ -bungarotoxin (T0195, 1/500) (Sigma-Aldrich). Lumbar MN were counted on six sections, interneurons on four sections, and serotonergic neurons on one coronal section (bregma –4.72mm). Approximately 100 NMJ were examined per animal. Images were captured using an AxioImager M2 microscope equipped with a structured illumination system (Apotome, Zeiss, Oberkochen, Germany) and a high-resolution B/W camera (Hamamatsu, Iwata, Shizuoka, Japan), and run by the ZEN 2 software (Zeiss).

### Statistical Analysis

Data are presented as the mean  $\pm$  SEM. Analyses were performed in GraphPad Prism v.6 (GraphPad Software, San Diego, CA), using Student *t* test, 1-way and 2-way analysis of variance (ANOVA), followed by Tukey's multiple comparisons post hoc test, the log-rank test (Mantel–Cox), Grubbs' test and Fischer's exact test. Results were considered significant when  $p < 0.05$ .

## Results

### Generation of the *Fezf2*<sup>-/-</sup>; *Sod1*<sup>G86R</sup> Mice

To test the contribution of the cerebral cortex to ALS, we generated a mouse line overexpressing the mutant *Sod1*<sup>G86R</sup> transgene but lacking SubCerPN, by crossbreeding *Sod1*<sup>G86R</sup> to *Fezf2*<sup>-/-</sup> mice. We obtained four genotypes: *Fezf2*<sup>+/+</sup> and non-transgenic (*WT*), *Fezf2*<sup>-/-</sup> and non-transgenic (*KO*), *Fezf2*<sup>+/+</sup> and *Sod1*<sup>G86R</sup> (*Sod1*), and *Fezf2*<sup>-/-</sup> and *Sod1*<sup>G86R</sup> (*KO/Sod1*) (Fig 1). Fluorogold injection into the cervical portion of the dorsal funiculus confirmed the absence of retrogradely labeled CSN, a subpopulation of SubCerPN, in the motor cortex of *KO* mice compared with *WT*. Immunostaining of CTIP2 further confirmed the absence of layer V SubCerPN in *KO* and *KO/Sod1* animals compared with their *WT* and *Sod1* littermates. To verify that absence of *Fezf2* expression had no effect on *Sod1* expression or on spinal MN generation, we ran qPCR analyses. Upregulation of *Sod1* expression was verified in *Sod1* and *KO/Sod1* animals and did not differ between the two genotypes, neither in the cerebral cortex nor in the spinal cord. Expression of the motoneuronal marker *Chat* was not significantly different between any of the four genotypes. Together, the data suggest that *KO/Sod1* mice represent a good model to study the impact of SubCerPN on the onset and progression of the ALS-like phenotype, and to test the corticofugal hypothesis.

### Absence of SubCerPN Delays Disease Onset and Death

To examine the consequences of the absence of projections from the cerebral cortex to its main subcerebral targets, we followed *Sod1* and *KO/Sod1* mice and their controls (Fig 2). The 75-day-old *KO* and *KO/Sod1* mice were lighter than *WT* and *Sod1* mice, but their body mass index was comparable (data not shown), indicating that *KO* and *KO/Sod1* mice were smaller but not thinner than their *WT* and *Sod1* littermates. As opposed to *WT* and *KO* mice, *Sod1* and *KO/Sod1* mice prematurely stopped gaining weight. Using weight peak as the disease onset, we observed that *KO/Sod1* mice presented a significant delay of disease onset compared with their *Sod1* littermates (median: 107.5 vs 159 days;  $p = 0.0070$ ). Likewise, survival of the *KO/Sod1* mice was increased compared with that of *Sod1* mice (median: 130 vs 183 days;  $p = 0.0083$ ), but the overall disease duration was not significantly different. Finally, the weight loss during the course of the disease was significantly smaller for the *KO/Sod1* mice than for the *Sod1* mice ( $36.45 \pm 1.82$  vs  $25.07 \pm 1.68\%$ ;  $p < 0.0001$ ), in accordance with an arrest of weight gain rather than a clear weight loss and an increased survival.

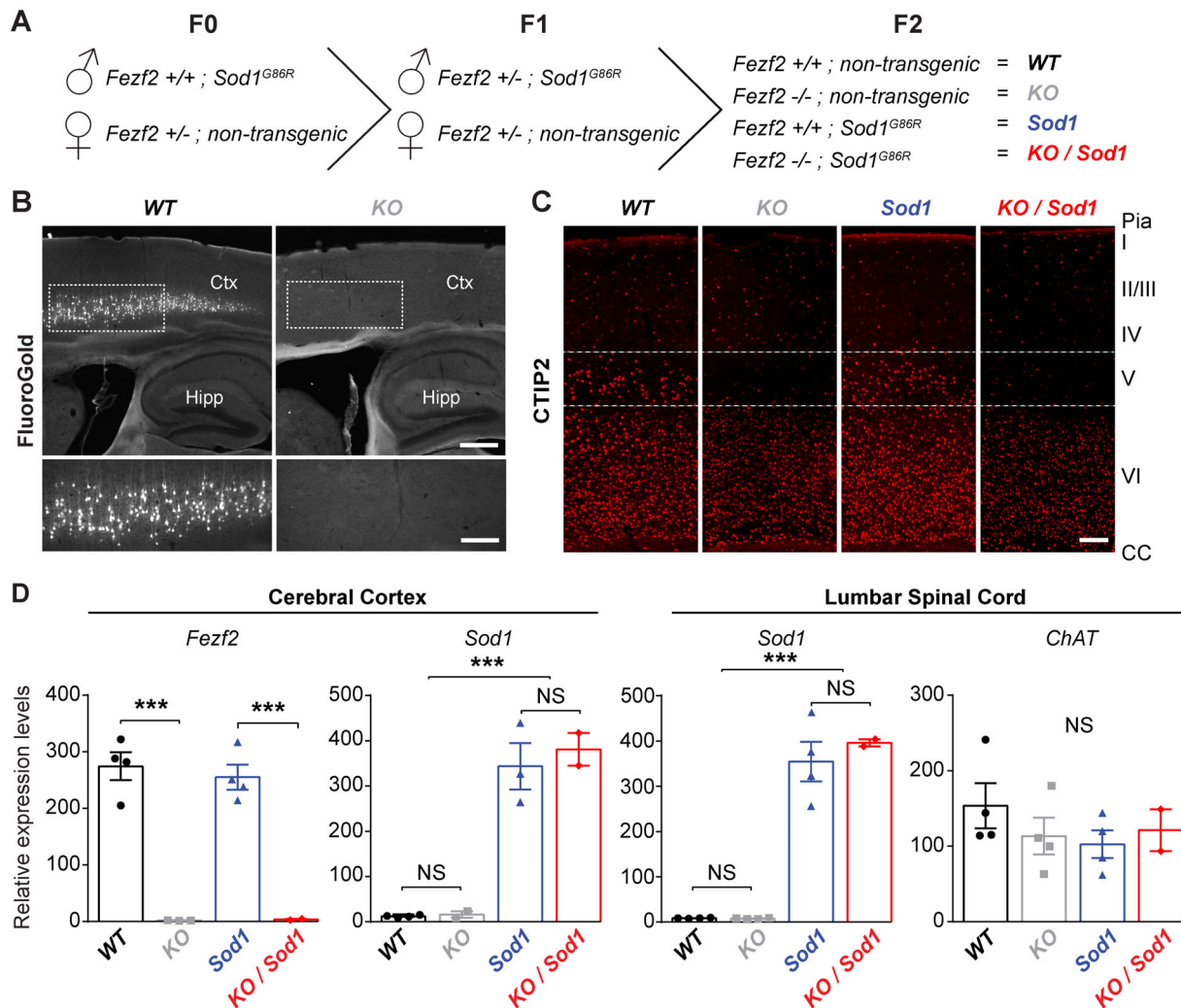


**FIGURE 1:** Generation of a mouse model overexpressing the *Sod1*<sup>G86R</sup> transgene but lacking all subcerebral projection neurons (SubCerPN), including the corticospinal neurons (CSN). (A) Schematic diagram of the crossbreeding of the *Sod1*<sup>G86R</sup> and *Fezf2*<sup>-/-</sup> mouse lines to generate four genotypes of interest: WT, KO, *Sod1*, and *KO/Sod1*. (B) Retrograde labeling of the CSN from the spinal cord of KO animals (right) and WT (left), showing absence of CSN in KO mice. *n* = 5 for all genotypes. (C) Representative images of brain coronal sections, at the level of the motor cortex, showing CTIP2 immunolabeling of layer V SubCerPN and of layer VI corticothalamic projection neurons (CThPN) in WT and *Sod1* mice, and confirming the absence of cortical layer V SubCerPN from the KO and *KO/Sod1* animals. *n* = 3 for all genotypes. (D) Quantitative PCR analysis of *Fezf2*, *Sod1*, and *Chat* expression in the cerebral cortex and spinal cord of 75-day-old animals, indicating that absence of *Fezf2* does not affect *Sod1* or *Chat* expression; 2-way ANOVA; *n* = 4 WT, *n* = 4 KO, *n* = 4 *Sod1*, and *n* = 2 *KO/Sod1*; \*\*\**p* < 0.001. Scale bars: 400μm in upper panels and 200μm in lower panels of B; and 250μm in C. [Color figure can be viewed at [www.annalsofneurology.org](http://www.annalsofneurology.org)]

Together, the data indicate that in the *Sod1*<sup>G86R</sup> mouse model of ALS the absence of SubCerPN is beneficial.

### Absence of SubCerPN Attenuates Motor Impairment

Next, we tested whether absence of SubCerPN could ameliorate motor performances and used linear regression analysis with the weight as a covariable to compare the animals both at the beginning and over the course of the experiment (origin and slope, respectively; Table S1). On the grip test and rotarod, *Sod1* and *KO/Sod1* mice rapidly showed reduced performances, but *KO/Sod1* mice were

affected later than their *Sod1* littermates and maintained higher performances over time than their *Sod1* littermates (Fig 2). On the inverted grid, *KO* and *KO/Sod1* mice initially displayed more difficulties in opposing their gravitational force compared with WT and *Sod1* mice. Yet, although WT and KO animals maintained their hanging time throughout all the repetitive assessments, *Sod1* and *KO/Sod1* gradually decreased their performances. However, this decrease occurred later and in a more moderate manner in *KO/Sod1* versus *Sod1* animals.

Linear regression analyses of the gait recorded on a CatWalk device using weight and speed as covariates

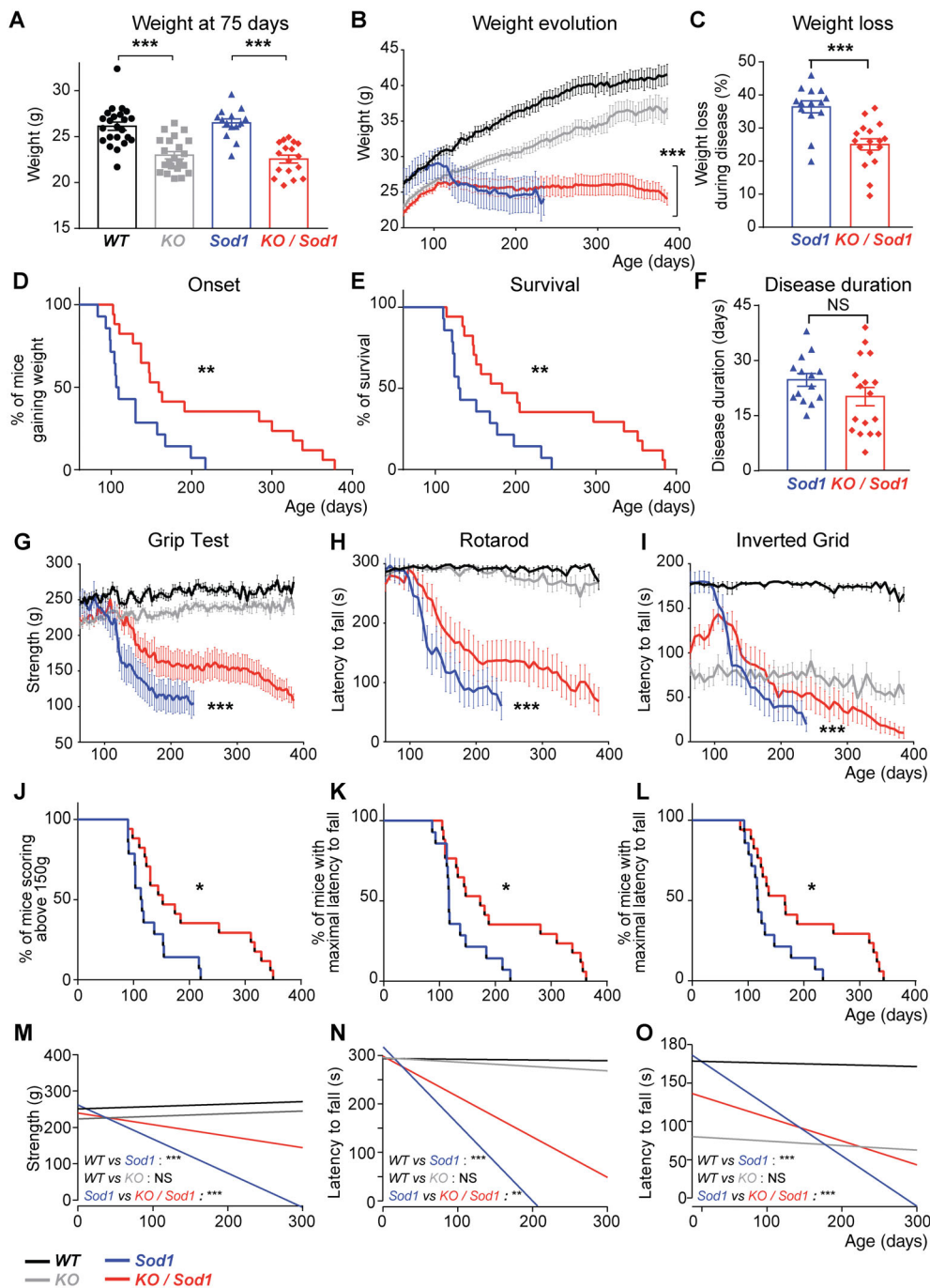


**FIGURE 2: Absence of subcerebral projection neurons (SubCerPN) delays onset, prevents weight loss, prolongs survival, and slows the decline of motor capacities. (A)** Bar graph representing the average weight of the four groups of mice at the beginning of the survival study (75 days); 1-way ANOVA. **(B)** Graphical representation of the evolution of the weight over time for the four genotypes. Note that although *Sod1* mice clearly lost weight, *KO/Sod1* mice instead stopped gaining weight; linear mixed effects model. **(C)** Bar graph representing the percentage of weight lost throughout the course of the disease; Student unpaired t test. **(D, E)** Kaplan–Meier plots of disease onset, defined as the time when animals stopped gaining weight (D), and survival (E) in days, for *Sod1* and *KO/Sod1* mice; log-rank test (Mantel–Cox). **(F)** Bar graph representing disease duration in days; Student unpaired t test. **(G–I)** Graphical representation of motor capacities over time, in days, on the grip strength test (G), the rotarod test (H), and the inverted grid test (I); linear mixed effects model. **(J–L)** Kaplan–Meier plots of grip strength score >150g (J) and maximal latency to fall from the rotarod (K) or from the inverted grid (L); log-rank test (Mantel–Cox). **(M–O)** Linear regression analysis conducted using the weight as covariate; the comparisons represented here are those of the slopes. For all data, n = 23 WT, n = 22 KO, n = 14 *Sod1*, and n = 17 *KO/Sod1*; \*p < 0.05, \*\*p < 0.01, \*\*\*p < 0.001; NS, nonsignificant.

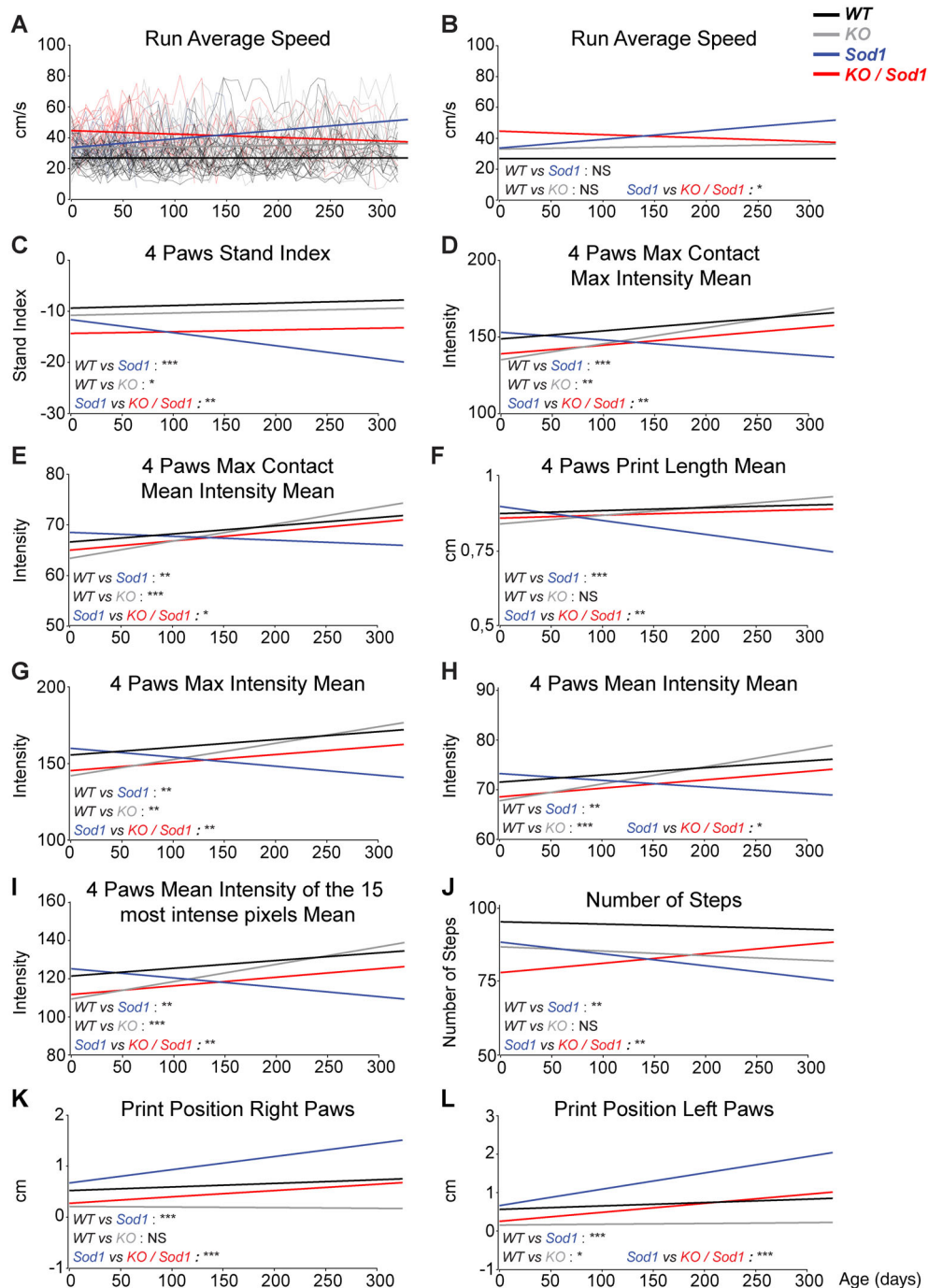


**FIGURE 3: Absence of subcerebral projection neurons (SubCerPN) ameliorates gait parameters recorded on CatWalk. (A–L)** Linear regression analyses were used to model overall evolution of the groups of animals, taking into account the individual progressions of each mouse over time. Weight was used as a covariate in A and B, and weight and speed were used as covariates in C–L. Individual mouse traces were removed from B–L to ease visualization of the regression curves (compare B with A). The comparisons represented here are those of the slopes. For all data,  $n = 23$  WT,  $n = 22$  KO,  $n = 14$  *Sod1*, and  $n = 17$  *KO/Sod1*; \* $p < 0.05$ , \*\* $p < 0.01$ , \*\*\* $p < 0.001$ ; NS, nonsignificant.

identified 3 parameters significantly different between *WT* and *KO* animals over time, and not between *WT* and *Sod1* animals, probably reflecting the consequences of the absence of CSN (*WT* versus *KO*; see Table S1). We also identified 15 parameters significantly altered in *Sod1* versus *WT* mice during disease progression (see Table S1).

Amongst them, 10 were also significantly different in *Sod1* versus *KO/Sod1* animals (Fig 3). Of those, two parameters showed opposite effects between absence of *Fesf2* and overexpression of *Sod1*<sup>G86R</sup>, whereas eight parameters instead showed a genuine amelioration of the *Sod1* phenotype in the absence CNS (*KO/Sod1* vs *Sod1*). Overall,

CatWalk analysis indicated that the absence of CSN ameliorated a set parameters affected in *Sod1*<sup>G86R</sup> animals as disease progressed. Together, the data confirmed the beneficial effects of the absence of SubCerPN on motor impairment in *Sod1*<sup>G86R</sup> mice.

#### **Absence of CSN Minimizes Spinal MN Loss and Neuromuscular Junction Denervation without Modifying Other Pathological Hallmarks of ALS**

We also investigated the spinal cord of end-stage animals, for its relevance to ALS but also as the target of CSN. Staining for GFAP and IBA1 revealed astrogliosis and microgliosis in the lumbar spinal cord of *Sod1* and *KO/Sod1* animals, without any difference between the two genotypes (Fig 4). Labeling of the autophagy marker P62/SQTM1 revealed a healthy, homogeneous cytoplasmic staining in both *WT* and *KO* mice and large, stellate-like inclusions in *Sod1* and *KO/Sod1* mice, with similar occurrence and intensity. Immunolabeling and counting of the ChAT<sup>+</sup> MN revealed a mild decrease of their somas in *Sod1* mice, as reported,<sup>21</sup> and maintenance of a bigger pool of MN in *KO/Sod1* versus *Sod1* animals ( $8.456 \pm 0.49$  vs  $6.152 \pm 0.57$ ;  $p = 0.0306$ ). Neuromuscular junction (NMJ) labeling and rating indicated that *KO/Sod1* animals had 2 times as many innervated NMJ as *Sod1* animals by disease end-stage ( $23.8 \pm 4.87\%$  vs  $11.34 \pm 3.12\%$ ;  $p = 0.0239$ ). Overall, the data show that the absence of cortical afferents to the spinal cord partly protects against Wallerian degeneration of the MN without modifying levels of spinal gliosis and dysregulation of autophagy.

#### **Neither *Sod1*<sup>G86R</sup> Overexpression nor Absence of SubCerPN Modifies TDP-43 Subcellular Localization**

The corticofugal hypothesis of ALS was proposed upon staging of the TDP-43 pathology.<sup>6,7</sup> Although TDP-43 aggregates have not been reported in *SOD1* ALS patients,<sup>24</sup> their putative occurrence in *Sod1*<sup>G86R</sup> mice has, to our knowledge, not been evaluated. To test whether increased survival and partial protection of MN in *KO/Sod1* animals was correlated with altered TDP-43 subcellular localization, we performed immunolabeling on end-stage animals and controls. Colocalization analyses in CRYM<sup>+</sup> SubCerPN of the motor cortex of *WT* and *Sod1* animals indicated that *Sod1*<sup>G86R</sup> overexpression was not associated with nuclear depletion of TDP-43 or occurrence of TDP-43<sup>+</sup> aggregates (Fig 5). No difference in TDP-43 immunoreactivity could be observed in the surrounding cortical environment either. In the spinal cord, we failed to detect any difference in TDP-43 immunoreactivity in CHAT<sup>+</sup> MN or in their surrounding

environment across genotypes. Together, the data suggest that in the *Sod1*<sup>G86R</sup> mouse model of ALS, the detrimental message carried along the corticofugal tracts probably does not take the form of TDP-43<sup>+</sup> aggregates.

#### **Absence of CSN Positively Impacts Hyper-Reflexia but Not Spasticity**

In humans, degeneration or lesion of the corticospinal tract results in appearance of the upper motoneuron syndrome,<sup>25</sup> a series of signs that include muscular weakness, decreased motor control, hyper-reflexia, including spasticity, and clonus.<sup>26</sup> In ALS patients, spasticity is typically evaluated using the modified Ashworth Scale, which measures the resistance to a passive soft-tissue stretching performed by the physician.<sup>27</sup> Hyper-reflexia instead is observed clinically as a hyperactive deep tendon reflex and electrophysiologically as an increase of the monosynaptic spinal reflex activity revealed by an increase of the ratio between the short-latency Hoffman's reflex, or H-reflex, to compound muscle action potentials (H/M ratio).<sup>28</sup> In rodents, assessment of the tail long lasting reflex (LLR) after cutaneous stimulation is accepted as a simple method to assess spasticity in awake animals,<sup>29</sup> and the H/M ratio is used to evaluate hyper-reflexia and is correlated with spasticity.<sup>29,30</sup> We reasoned that the mouse line that we generated could contribute to evaluate the role of CSN in the modulation of spinal network excitability involved in hyper-reflexia and spasticity in an ALS-related context.

We ran electromyographic analyses on presymptomatic anesthetized mice to detect the H-reflex upon stimulation of the sciatic nerve and recording of the abductor digiti minimi muscle. We detected an H-reflex in fractions of *Sod1* and *KO/Sod1* groups of animals, but never in the *WT* or *KO* animals (Fig 6). Thus, the H-reflex developed only in *Sod1*<sup>G86R</sup> animals, independently of the presence of CSN and, counterintuitively, the absence of CSN, per se, was not sufficient to trigger an H-reflex. Evaluation of the proportions of animals presenting an H-reflex did not reveal any significant difference between *Sod1* and *KO/Sod1* at this age. However, measurement of the H/M ratio among the animals displaying an H-reflex showed a significant reduction in *KO/Sod1* animals compared with their *Sod1* littermates. This suggests that, at presymptomatic ages, absence of CSN limits hyper-reflexia. To further evaluate spasticity, we assessed the tail LLR in awake and fully paralyzed (end-stage) animals.<sup>22,29,31</sup> *Sod1* and *KO/Sod1* animals could be subdivided into spastic and nonspastic, but the relative proportions of each or intensity of the response to the stimulation were not significantly different between *Sod1* and *KO/Sod1* mice, suggesting that absence of CSN is not sufficient to prevent the manifestation of spasticity in

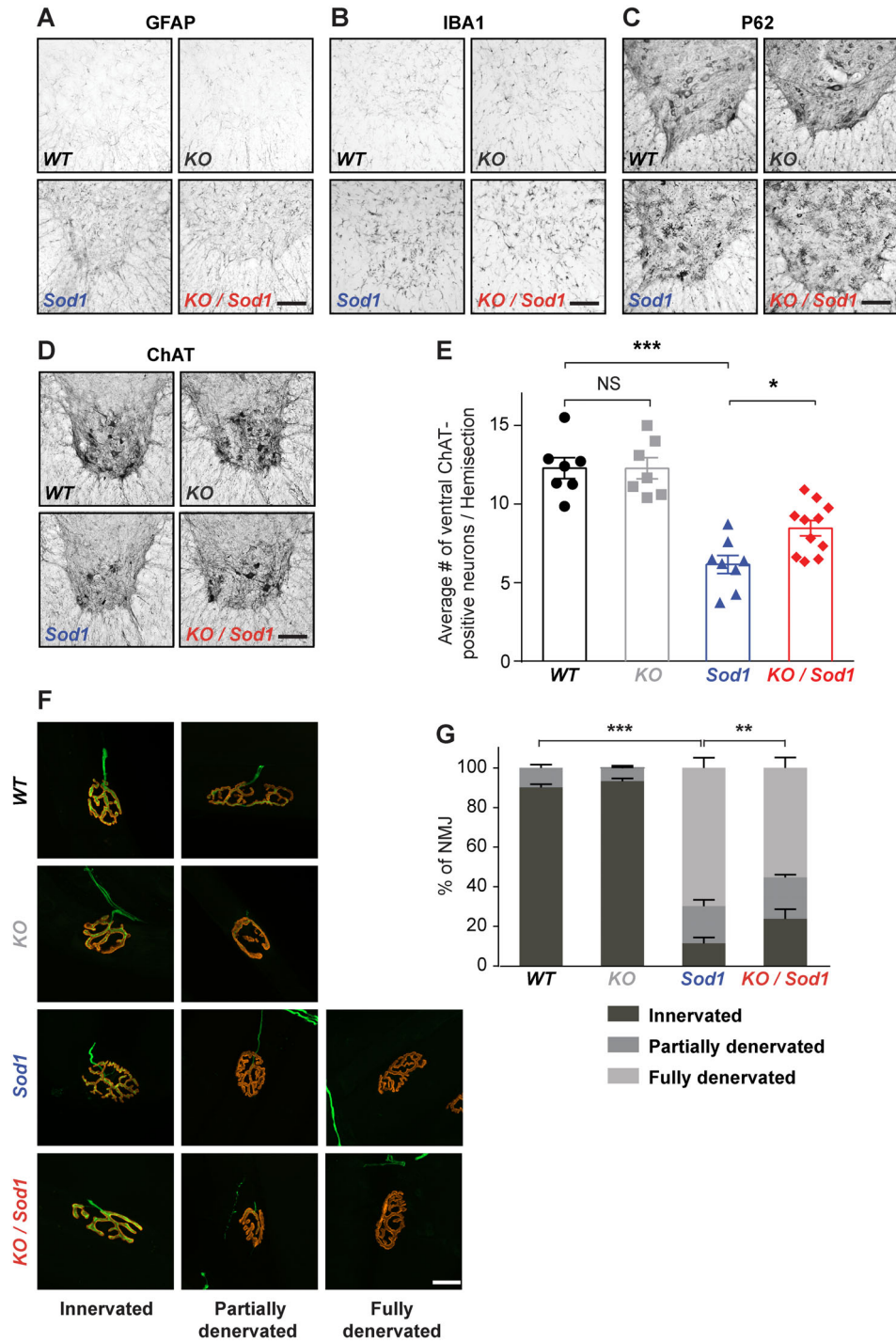


**FIGURE 4: Absence of corticospinal neurons (CSN) partly prevents degeneration of the motoneuron (MN) cell bodies and neuromuscular junction (NMJ) dismantlement. (A–D)** Representative immunostaining images of the ventral horn of the lumbar spinal cord from end-stage *Sod1* and *KO/Sod1* mice and their age-matched *WT* and *KO* littermates labeled with GFAP (A), IBA1 (B), P62 (C), and choline acetyltransferase (ChAT; D). (E) Bar graph representing the average number of ventral ChAT<sup>+</sup> neurons per lumbar spinal cord hemi-section; 1-way ANOVA; n = 6 *WT*, n = 6 *KO*, n = 8 *Sod1*, and n = 10 *KO/Sod1*. (F) Representative maximum-intensity projection images of z-stacks of typically innervated, partly or fully denervated NMJs from end-stage *Sod1* and *KO/Sod1* mice and their age-matched *WT* and *KO* littermates. (G) Bar graph representing the average proportions of innervated (dark gray), partly denervated (medium gray) and fully denervated (light gray) NMJs for each genotype; 2-way ANOVA followed by Tukey multiple comparisons test; n = 6 animals per genotype. \*\*p < 0.05, \*\*\*p < 0.01, \*\*\*\*p < 0.001; NS, nonsignificant. Scale bars: 100µm in A–D; 20µm in F. [Color figure can be viewed at [www.annalsofneurology.org](http://www.annalsofneurology.org)]



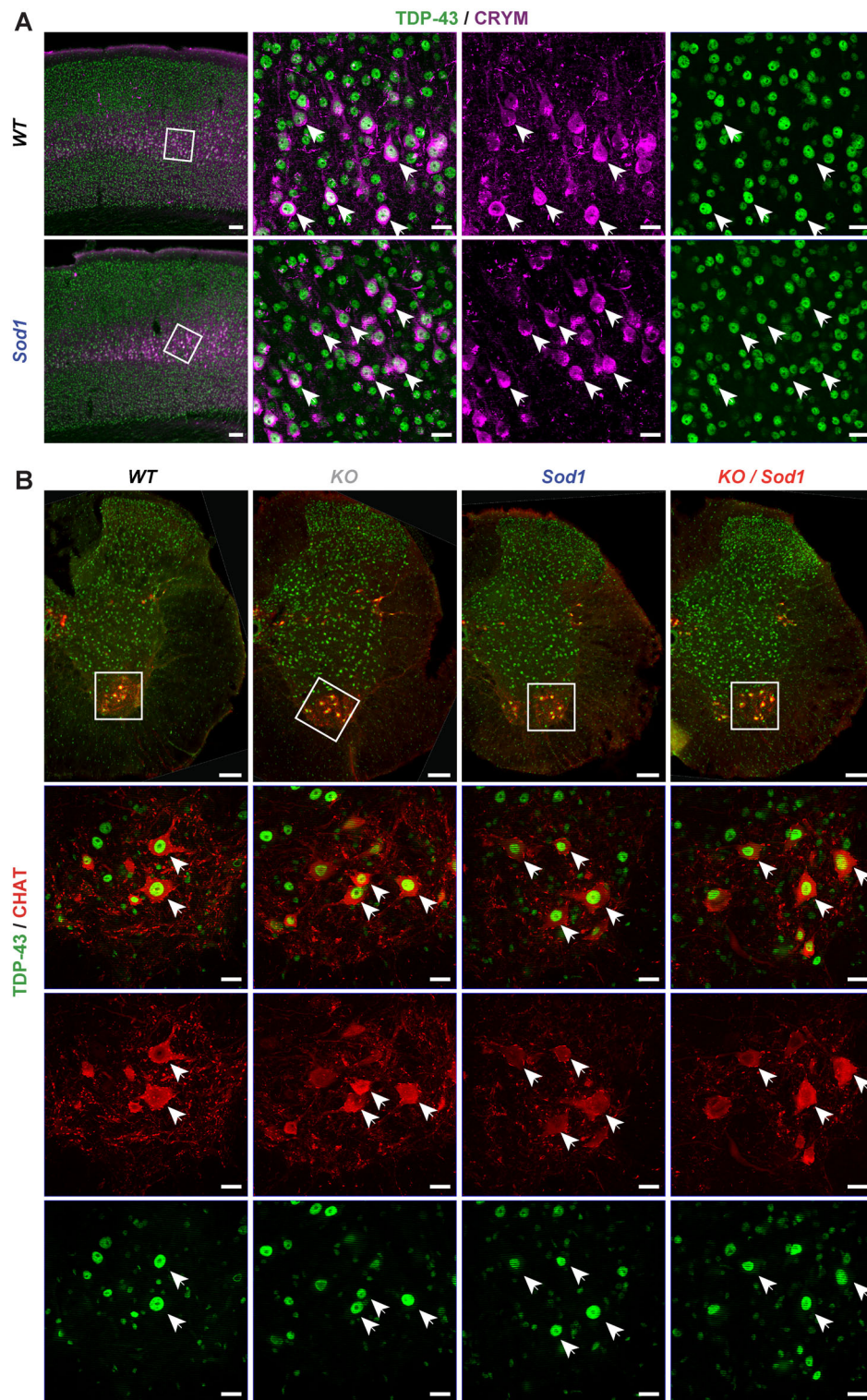


**FIGURE 5:** TDP-43 subcellular localization is not modified in the absence of subcerebral projection neurons (SubCerPN) or with the expression of *Sod1*<sup>G86R</sup>. (A) Representative images of coronal sections of the motor cortex of end-stage *Sod1* and age-matched *WT* mice, showing nuclear localization of TDP-43<sup>+</sup> (green) in CRYM<sup>+</sup> (purple) SubCerPN. (B) Representative images of lumbar spinal cord hemisections of *Sod1* and *KO/Sod1* mice at end-stage and their age-matched *WT* and *KO* littermates, showing nuclear TDP-43 (green) within ChAT<sup>+</sup> (red) motoneurons. *n* = 5 per genotype. Scale bar: 100 and 20 $\mu$ m in close-ups.

end-stage animals. Together, the data indicate that hyper-reflexia arises presymptomatically in *Sod1*<sup>G86R</sup> mice and that absence of CSN decreases this particular feature of spasticity. In contrast, spasticity assessed by LLR in end-stage *Sod1*<sup>G86R</sup> animals does not appear to be modulated by CSN. In addition to the absence or the gradual loss of CSN, other mechanisms might account for the occurrence of hyper-reflexia and spasticity in mice.

### End-Stage Spasticity is Correlated with Loss of Serotonergic Neurons and of Recurrent Inhibition onto MN

Emergence of spasticity could arise from altered supraspinal controls, and more particularly serotonergic inputs, and from spinal network rearrangements.<sup>22,31–33</sup> We thus tested whether absence of SubCerPN could affect the population of TPH2<sup>+</sup> neurons present in the raphe

nuclei throughout the course of the disease in *Sod1* and *KO/Sod1* animals compared with controls (Fig 7). As reported,<sup>31</sup> end-stage *Sod1* mice displayed significant loss of TPH2<sup>+</sup> neurons compared with *WT*. Likewise, we observed significant loss of TPH2<sup>+</sup> neurons in end-stage *KO/Sod1* mice compared with *WT*, but no significant difference between *Sod1* and *KO/Sod1* animals. At younger ages, no significant difference could be detected across the different groups of mice. Together, the data indicate that absence of CSN and other SubCerPN does not affect survival of the serotonergic neurons and that occurrence of LLR in end-stage animals could, at least in part, result from the late loss of serotonergic neurons.

To determine whether absence of CSN could affect the populations of inhibitory spinal IN in *KO* and *KO/Sod1* animals compared with controls, we labeled and quantified parvalbumin- (PV), calretinin- (CR) and

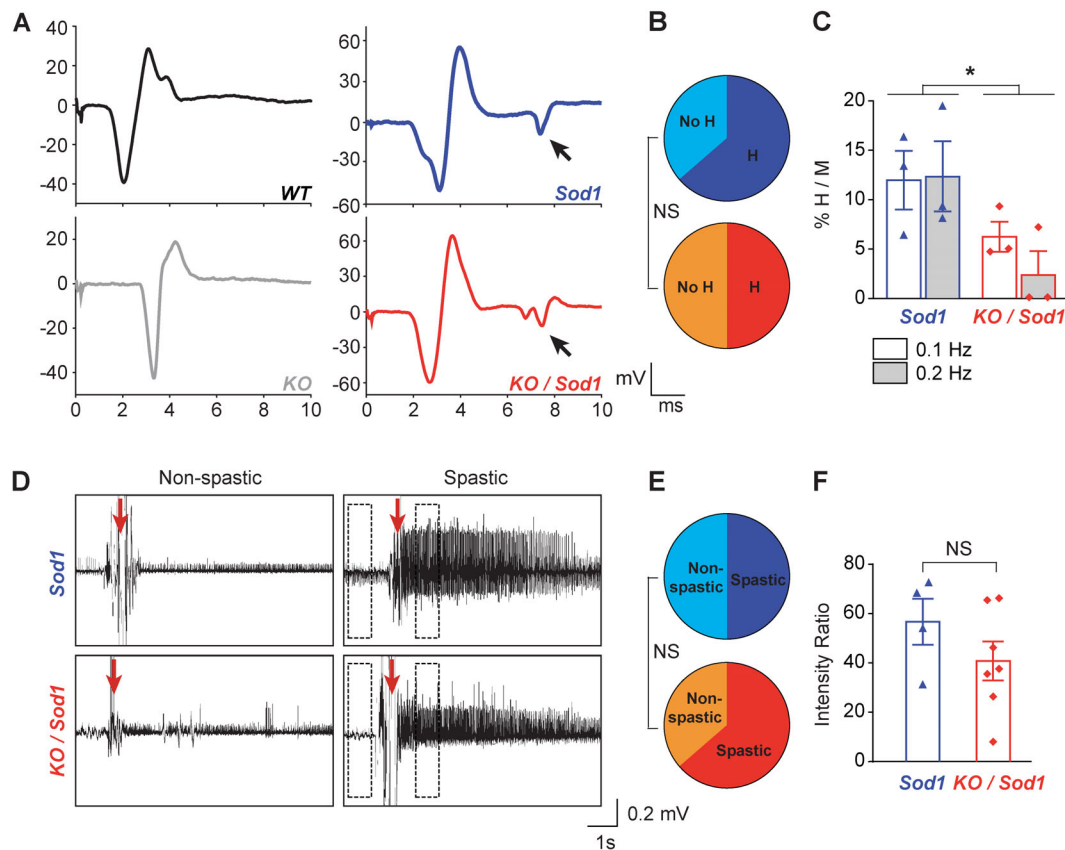


**FIGURE 6: Absence of corticospinal neurons (CSN) minimizes presymptomatic hyper-reflexia but not end-stage spasticity.** (A) Representative electromyographic traces of the muscular response of the abductor digiti minimi muscle upon sciatic nerve stimulation. Arrows indicate H-reflex in presymptomatic *Sod1* and *KO/Sod1* mice;  $n = 6$  *WT*,  $n = 6$  *KO*,  $n = 8$  *Sod1*, and  $n = 10$  *KO/Sod1*. (B) Pie charts representing the percentage of animals with an H-reflex amongst *Sod1* (top) and *KO/Sod1* (bottom) animals; Fischer exact test. (C) Bar graph representing the averaged ratios of the amplitude of the H-reflex and M-wave upon repeated stimulations at 0.1 and 0.2 Hz, in *Sod1* and *KO/Sod1* mice;  $n = 3$  *Sod1* and  $n = 3$  *KO/Sod1*; 2-way ANOVA. (D) Representative electromyographic recordings of the tail muscle upon stimulation of end-stage, fully paralyzed and awake *Sod1* mice. Spasticity-related tail long-lasting reflex (LLR; right panels) can be observed upon stimulation (red arrow) in subgroups of animals. (E) Pie charts representing the percentage with an LLR amongst *Sod1* (top) and *KO/Sod1* (bottom) animals; Fischer exact test;  $n = 8$  *Sod1* and  $n = 11$  *KO/Sod1*. (F) Signal-to-noise intensity ratios of the LLR calculated from measurements made in dotted boxes in D; Student unpaired t test;  $n = 4$  *Sod1* and  $n = 7$  *KO/Sod1*;  $*p < 0.05$ . [Color figure can be viewed at [www.annalsofneurology.org](http://www.annalsofneurology.org)]

calbindin- (CB) positive IN present in the lumbar spinal cord of 105-day-old and end-stage animals and their age-matched control littermates. The populations of PV<sup>+</sup> and CR<sup>+</sup> IN in laminae IV–IX were found to be unchanged across genotypes and ages (Fig 8A–D). In contrast, CB<sup>+</sup> IN present in the ventral horn of the spinal cord, which include the subpopulation of Renshaw cells that exert recurrent inhibition onto MN,<sup>34</sup> were decreased in end-stage *Sod1* and *KO/Sod1* animals in comparison to their *WT* and *KO* littermates ( $p = 0.0110$  between *KO* and *KO/Sod1* and  $p = 0.0900$  between *WT* and *Sod1*; see Fig 8E,F). Overall, the results indicate that the absence of CSN does not modify the populations of spinal inhibitory IN and that *Sod1*<sup>G86R</sup> transgene expression leads to a late loss of CB<sup>+</sup> IN, which could account for spasticity at late stages of the disease.

## Discussion

In this study, we demonstrated that absence of SubCerPN delayed disease onset, extended survival, and improved clinical conditions of a mouse model of ALS, providing the first experimental arguments in favor of the corticofugal hypothesis.

## Contribution of the Cerebral Cortex and its Outputs to ALS

Although the origin of ALS remains debated,<sup>2</sup> evidence from neurophysiological and pathological studies conducted on patients<sup>4,5</sup> are nourishing a revival of interest in Charcot's initial view of ALS as a primary cortical impairment.<sup>3</sup> Whether disease propagation relies on altered neuronal excitability and subsequent excitotoxicity<sup>5</sup> or on prion-like propagation of misfolded proteins,<sup>7</sup> both schools of thought agree on a common cortical origin and propagation along the corticofugal tracts.<sup>4</sup> However, the hypothesis cannot be tested directly in patients. Although the corticomotoneuronal system has undergone major modifications with evolution,<sup>4</sup> corticothalamic and SubCerPN populations are remarkably well conserved between mice and humans, as opposed to the commissural and associative projection neuron populations.<sup>35</sup> Further support for the appropriateness of rodents to study the cortical contributions to ALS is provided by their ability to recapitulate CSN or SubCerPN degeneration.<sup>8</sup> In the *Sod1*<sup>G86R</sup> mouse model, CSN precedes MN degeneration and NMJ denervation.<sup>11</sup> Thus, rodent models and *Sod1*<sup>G86R</sup> mice in particular seem suitable to assess the contribution of SubCerPN to ALS.

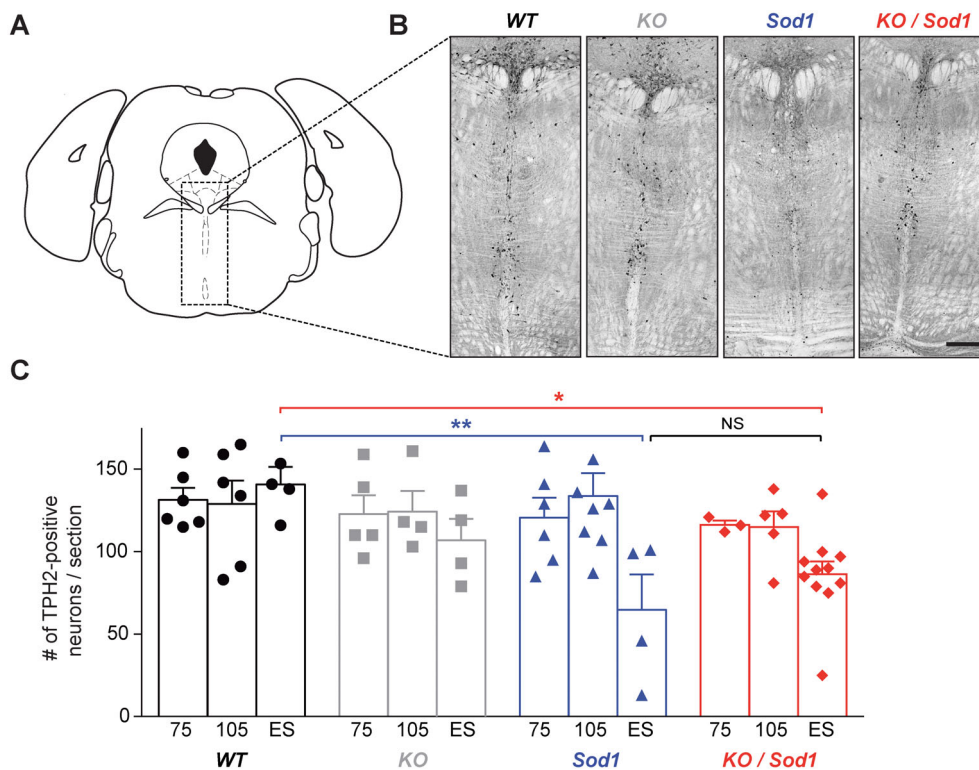


**FIGURE 7:** Absence of subcerebral projection neurons (SubCerPN) does not prevent the late loss of serotonergic neurons in the raphe nuclei. (A) Schematic diagram of the coronal section selected for TPH2<sup>+</sup> neuron labeling and counting. (B) Representative images of TPH2 immunoreactivity in the brainstem (dorsal and median raphe) of end-stage mice. (C) Bar graph representing the average number of TPH2<sup>+</sup> neurons, over time (75 and 105 days and end-stage [ES]), in WT (n = 6, 6, and 4, respectively), KO (n = 5, 4, and 4, respectively), *Sod1* (n = 6, 8, and 4, respectively), and *KO/Sod1* (n = 3, 5, and 11, respectively) mice; 2-way ANOVA followed by Tukey multiple comparisons test; \* $p < 0.05$ , \*\* $p < 0.01$ . Scale bar: 300 $\mu$ m. [Color figure can be viewed at [www.annalsofneurology.org](http://www.annalsofneurology.org)]

### Absence of SubCerPN Delays Onset and Extends Survival without Increasing Disease Duration

Crossbreeding of *Sod1*<sup>G86R</sup> and *Fezf2*<sup>-/-</sup> mouse lines generated animals ubiquitously expressing *Sod1*<sup>G86R</sup> but lacking SubCerPN, including CSN, hence challenging the definition of ALS. Absence of SubCerPN delayed disease

onset and increased survival without modifying disease duration. The results are highly reminiscent of an elegant study by Thomsen and colleagues,<sup>36</sup> who knocked down *SOD1*<sup>G93A</sup> in the posterior motor cortex of transgenic rats using AAV9–SOD1–shRNA injections and reported delayed disease onset, extended survival and unchanged disease duration. The similarity of these and our results is

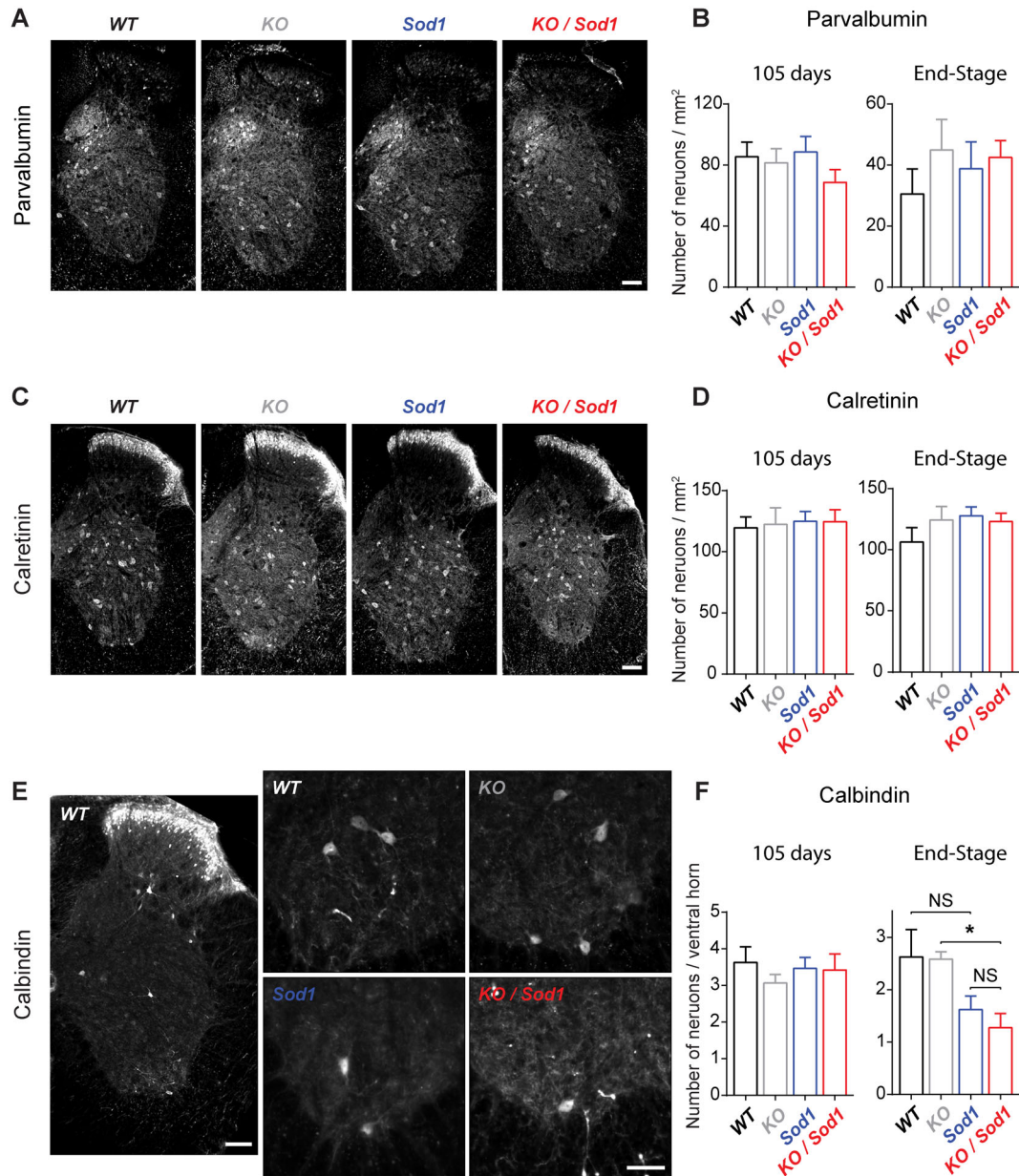


**FIGURE 8:** Population of Renshaw cells decreases in end-stage *Sod1* and *KO/Sod1* mice. (A, C, E) Representative images of lumbar spinal cord hemi-sections from end-stage *Sod1* and *KO/Sod1* mice and their age-matched WT and KO littermates labeled with parvalbumin (A), calretinin (C), and calbindin (E) antibodies. (B, D) Bar graphs representing the average number of parvalbumin-positive (B) or calretinin-positive (D) inhibitory interneurons (IN) per square millimeter in laminae IV–IX of lumbar spinal cord of 105-day-old and end-stage animals. (F) Bar graph representing the average number of calbindin-positive IN in the ventral horn of lumbar spinal cord of 105-day-old and end-stage animals. For 105-day-old and end-stage WT ( $n = 6$  and  $5$ , respectively), KO ( $n = 4$  and  $6$ , respectively), *Sod1* ( $n = 7$  and  $7$ , respectively), and *KO/Sod1* ( $n = 6$  and  $11$ , respectively); 1-way ANOVA followed by Tukey multiple comparisons test;  $*p < 0.05$ . Scale bars:  $100\mu\text{m}$  in A, C, and the left panel of E;  $50\mu\text{m}$  in the close-ups of E. [Color figure can be viewed at [www.annalsofneurology.org](http://www.annalsofneurology.org)]

remarkable given the differences in the approaches. Together, the two studies suggest that absence of diseased CSN or instead maintenance of genetically corrected CSN might be equally beneficial and that *Sod1/SOD1* mutant transgene-expressing CSN might be detrimental to their downstream targets. Yet, it is worth mentioning that AAV9 is likely to have targeted all types of cortical excitatory and inhibitory neurons, potentially contributing to correct cortical circuit dysfunctions such as those reported in *Sod1<sup>G93A</sup>* and *TDP-43<sup>A315T</sup>* mouse models of ALS.<sup>8</sup> Cell type-specific genetic ablation experiments could provide further information on the contribution of individual neuronal and glial populations to cortical circuit dysfunction and consequences for corticofugal targets. Such approaches allow better definition of the contributions of MN, microglia, astrocytes, and muscles to ALS onset and progression.<sup>37</sup> Together, these studies and ours indicate that the cerebral cortex and SubCerPN might be involved in disease onset, whereas MN and glia might modulate disease progression.

#### **Absence of CSN Improves Motor Performances and Minimizes MN Degeneration**

Although *Fezf2<sup>-/-</sup>* mice lack CSN and other SubCerPN and display altered cortical development,<sup>13,14,17</sup> they remarkably do not present any major motor phenotype. In mice, CSN make mostly indirect or polysynaptic connections and few direct or monosynaptic connections onto MN.<sup>38</sup> It is possible that in *Fezf2<sup>-/-</sup>* mice the majority of indirect connections are less affected, or better compensated, and the minority of direct connections are more affected but translate into a phenotype that is harder to reveal. In the *Celsr3/Emx1* mice, CST genetic ablation is correlated with increased numbers of rubrospinal and monoaminergic projections to the spinal cord.<sup>39</sup> Although the *Celsr3/Emx1* mice display proper locomotion, they show difficulties in fine motor tests.<sup>39</sup> In the present study, we found that *Fezf2<sup>-/-</sup>* mice, although smaller and lighter than controls, performed less well on the inverted grid test, possibly owing to defects in proper grip to the grid. In addition, the sensitive CatWalk gait analysis device revealed decreased performances of *Fezf2<sup>-/-</sup>* mice. Together, these data indicate that *Fezf2<sup>-/-</sup>* mice do present a discrete motor phenotype, which could possibly be further revealed by dedicated fine motor tests. Importantly, we found that absence of CSN and other SubCerPN improved the motor phenotype of the *Sod1<sup>G86R</sup>* mice and limited the denervation of the NMJ and ultimate loss of MN. This indicates that, although CSN might not be of great importance for locomotion in rodents, or their agenesis well compensated by other descending tracts, their presence in a context of ALS is

detrimental to their downstream MN targets, whether direct or indirect.

#### **Absence of CSN Limits Hyper-Reflexia**

Absence of SubCerPN in *Sod1<sup>G86R</sup>* mice ameliorated hyper-reflexia, a feature of the upper motoneuron syndrome.<sup>26</sup> The absence of H-reflex recording in *WT* animals does not rule out the existence of a small-amplitude H-reflex in these animals, below the detection threshold, as already observed.<sup>30</sup> In contrast, the presence of an H-reflex in subgroups of presymptomatic *Sod1* animals suggests that hyper-reflexia precedes the appearance of motor symptoms in these animals and is correlated with the presymptomatic degeneration of the CSN.<sup>11</sup> Absence of an H-reflex in *KO* animals suggests that developmental absence of CSN and other SubCerPN could have been compensated by other supraspinal controls or by spinal network rearrangements, or both. Finally, decreased H/M ratios in *KO/Sod1* compared with *Sod1* animals indicate decreased hyper-reflexia and possible mitigation of the upper motoneuron syndrome in the absence of CSN and other SubCerPN. In contrast, LLR of the tail muscle of fully paralyzed end-stage mice was neither prevented nor even slightly modulated by absence of SubCerPN. But given that evaluation of the LLR can be performed only in paralyzed animals, our study did not allow us to test whether spasticity could have arisen later in *KO/Sod1* than in *Sod1* mice. Supraspinal controls, and more particularly serotonergic inputs, and spinal network rearrangements could account for the emergence of spasticity.<sup>22,31–33</sup> We failed to detect any difference in TPH2<sup>+</sup> serotonergic neurons in the raphe nuclei and in PV<sup>+</sup>, CR<sup>+</sup>, and CB<sup>+</sup> inhibitory spinal IN at the time when presymptomatic hyper-reflexia was detected. However, an altered contribution of these neuronal populations to spinal circuits at this presymptomatic age could take the form of neuronal plasticity, which we did not test. At disease end-stage, we observed decreased amounts of serotonergic neurons in the raphe nuclei and of CB<sup>+</sup> IN in the ventral spinal cord of *Sod1* mice, in accordance with formerly published work,<sup>22,30,31,34</sup> and no difference between *Sod1* and *KO/Sod1* mice, suggesting that both mechanisms could account for the emergence of the LLR in these transgenic animals.

#### **Possible Propagation Mechanisms and Perspectives**

We demonstrated that absence of SubCerPN was beneficial in a mouse model of ALS, suggesting that major corticofugal projections might be detrimental to their downstream targets in the context of ALS. But whether corticofugal propagation of the disease relies on prion-like

transmission of misfolded proteins<sup>7</sup> or on altered neuronal excitability and subsequent excitotoxicity<sup>5</sup> remains an open question. As opposed to most ALS patients and like *SOD1* patients, *Sod1*<sup>G86R</sup> mice do not seem to present any TDP-43 pathology. However, they do present P62<sup>+</sup> aggregates, and the presence of misfolded proteins remains possible. Nevertheless, we did not observe any difference in P62 staining between *KO/Sod1* and *Sod1* animals that could be correlated with the extended survival of the double transgenic mice. In a recent study, we genetically ablated the *SOD1*<sup>G37R</sup> transgene from corticofugal projection neurons. This was sufficient to prevent CSN degeneration in a cell-autonomous manner but had no impact on disease onset and survival, ruling out a major contribution of misfolded protein propagation from the corticofugal neurons to their targets on disease occurrence and progression in this mouse model.<sup>40</sup> On the contrary, knock-down of the *SOD1*<sup>G93A</sup> mutant transgene in the posterior motor cortex of a rat model of ALS using AAV9 delayed disease onset and extended survival.<sup>36</sup> It is possible that this beneficial effect arose from targeting cortical IN that modulate the excitability and activity of corticofugal neurons.<sup>41</sup> Given the reported alterations in excitability of cortical neuron populations in different mouse models of the disease,<sup>8,42</sup> comparison between silencing and genetic ablation of adult corticofugal neurons would be particularly informative to gain a better understanding of the mechanism by which these neurons might contribute to disease onset and progression. Finally, deep molecular analysis of CSN dysfunction in ALS<sup>11</sup> might in the future provide a better understanding of the role of the cerebral cortex and its outputs to ALS and potentially unravel new therapeutic targets.

## Acknowledgment

The work has been supported by a European Research Council (ERC) starting grant (#639737), a Marie Skłodowska-Curie career integration grant (#618764), an “Association Française contre les Myopathies” (AFM)-Telethon trampoline grant (#16923), a “Fédération pour la Recherche sur le Cerveau” (FRC) grant, and a Neurex grant to C.R., PhD fellowships from the French Ministry of Research to T.B., C.B., and A.B., and from the “Association de Recherche sur la Sclérose Latérale Amyotrophique” (ARSLA) to C.B., and by a postdoctoral fellowship from the AFM-Telethon to J.C.Z. (#21993).

We are extremely thankful to Véronique Marchand-Pauvert, Pascal Branchereau, Pierre Veinante, and Luc Dupuis for critical reading of the manuscript and insightful comments.

## Author Contributions

T.B., C.B., M.C.-E., and C.R. contributed to the conception and design of the study; all authors contributed to the acquisition and analysis of the data; T.B., C.B., F.L., M.C.-E., and C.R. contributed to drafting the text and preparing the figures.

## Potential Conflicts of Interest

Nothing to report.

## References

1. Brown RH, Al-Chalabi A. Amyotrophic lateral sclerosis. *N Engl J Med* 2017;377:162–172.
2. Ravits JM, La Spada AR. ALS motor phenotype heterogeneity, focality, and spread. *Neurology* 2009;73:805–811.
3. Charcot JM. *Sclérose latérale amyotrophique: oeuvres complètes*. Paris: Bureaux du Progrès Medical, 1874.
4. Eisen A, Braak H, Del Tredici K, et al. Cortical influences drive amyotrophic lateral sclerosis. *J Neurol Neurosurg Psychiatry* 2017; 88:917–924.
5. Vucic S, Kiernan MC. Transcranial magnetic Stimulation for the assessment of neurodegenerative disease. *Neurotherapeutics* 2017; 14:91–106.
6. Brettschneider J, Del Tredici K, Toledo JB, et al. Stages of pTDP-43 pathology in amyotrophic lateral sclerosis. *Ann Neurol* 2013;74: 20–38.
7. Braak H, Brettschneider J, Ludolph AC, et al. Amyotrophic lateral sclerosis—a model of corticofugal axonal spread. *Nat Rev Neurol* 2013;9:708–714.
8. Brunet A, Stuart-Lopez G, Burg T, et al. Cortical circuit dysfunction as a potential driver of amyotrophic lateral sclerosis. *Front Neurosci* 2020;14:363.
9. Mancinelli S, Lodato S. ScienceDirectDecoding neuronal diversity in the developing cerebral cortex: from single cells to functional networks. *Curr Opin Neurobiol* 2018;53:146–155.
10. Tomassy GS, Lodato S, Trayer-Gibson Z, Arlotta P. Development and regeneration of projection neuron subtypes of the cerebral cortex. *Sci Prog* 2010;93:151–169.
11. Marques C, Fischer M, Keime C, et al. Early alterations of RNA metabolism and splicing from adult corticospinal neurons in an ALS mouse model. *bioRxiv* 2019. <https://doi.org/10.1101/667733>.
12. Zhang Q, Mao C, Jin J, et al. Side of limb-onset predicts laterality of gray matter loss in amyotrophic lateral sclerosis. *Biomed Res Int* 2014;2014:1–11.
13. Hirata T, Suda Y, Nakao K, et al. Zinc finger gene-like functions in the formation of subplate neurons and thalamocortical axons. *Dev Dyn* 2004;230:546–556.
14. Molyneaux BJ, Arlotta P, Hirata T, et al. Fez1 is required for the birth and specification of corticospinal motor neurons. *Neuron* 2005;47: 817–831.
15. Rouaux C, Arlotta P. Direct lineage reprogramming of post-mitotic callosal neurons into corticofugal neurons in vivo. *Nat Cell Biol* 2013; 15:214–221.
16. Rouaux C, Arlotta P. Fezf2 directs the differentiation of corticofugal neurons from striatal progenitors in vivo. *Nat Neurosci* 2010;13: 1345–1347.

17. Lodato S, Rouaux C, Quast KB, et al. Excitatory projection neuron subtypes control the distribution of local inhibitory interneurons in the cerebral cortex. *Neuron* 2011;69:763–779.
18. Ripps ME, Huntley GW, Hof PR, et al. Transgenic mice expressing an altered murine superoxide dismutase gene provide an animal model of amyotrophic lateral sclerosis. *PNAS* 1995;92:689–693.
19. Burg T, Bichara C, Scekcic-Zahirovic J, et al. Absence of subcerebral projection neurons delays disease onset and extends survival in a mouse model of ALS. *bioRxiv* 2019. <https://doi.org/10.1101/849935>.
20. Scekcic-Zahirovic J, Oussini El H, Mersmann S, et al. Motor neuron intrinsic and extrinsic mechanisms contribute to the pathogenesis of FUS-associated amyotrophic lateral sclerosis. *Acta Neuropathol* 2017;133:887–906.
21. Rouaux C, Panteleeva I, Rene F, et al. Sodium valproate exerts neuroprotective effects in vivo through CREB-binding protein-dependent mechanisms but does not improve survival in an amyotrophic lateral sclerosis mouse model. *J Neurosci* 2007;27:5535–5545.
22. Oussini El H, Scekcic-Zahirovic J, Verduyck P, et al. Degeneration of serotonin neurons triggers spasticity in amyotrophic lateral sclerosis. *Ann Neurol* 2017;82:444–456.
23. Lee S, Toda T, Kiyama H, Yamashita T. Weakened rate-dependent depression of Hoffmann's reflex and increased motoneuron hyperactivity after motor cortical infarction in mice. *Cell Death Dis* 2014; e1007:1–9.
24. Mackenzie IRA, Bigio EH, Ince PG, et al. Pathological TDP-43 distinguishes sporadic amyotrophic lateral sclerosis from amyotrophic lateral sclerosis with SOD1 mutations. *Ann Neurol* 2007;61:427–434.
25. Purves D, Augustine GJ, Fitzpatrick D, et al. *Neuroscience*. Sunderland, MA: Sinauer Associates, Inc, 2004.
26. Ivanhoe CB, Reistetter TA. Spasticity. *Am J Phys Med Rehabil* 2004; 83:S3–S9.
27. Ashworth NL, Satkunam LE, Deforge D. Treatment for spasticity in amyotrophic lateral sclerosis/motor neuron disease. *Cochrane Database Syst Rev* 2012;2:CD004156.
28. Simon NG, Lin CSY, Lee M, et al. Segmental motoneuronal dysfunction is a feature of amyotrophic lateral sclerosis. *Clin Neurophysiol* 2015;126:828–836.
29. Bennett DJ, Gorassini M, Sanelli L, et al. Spasticity in rats with sacral spinal cord injury. *J Neurotrauma* 1999;16:69–84.
30. Modol L, Mancuso R, Ale A, et al. Differential effects on KCC2 expression and spasticity of ALS and traumatic injuries to motoneurons. *Front Cell Neurosci* 2014;8:7.
31. Dentel C, Palamiuc L, Henriques A, et al. Degeneration of serotonergic neurons in amyotrophic lateral sclerosis: a link to spasticity. *Brain* 2013;136:483–493.
32. Martin LJ, Chang Q. Inhibitory synaptic regulation of motoneurons: a new target of disease mechanisms in amyotrophic lateral sclerosis. *Mol Neurobiol* 2011;45:30–42.
33. Mukherjee A, Chakravarty A. Spasticity mechanisms – for the clinician. *Front Neurol* 2010;1:149.
34. Wootz H, FitzSimons-Kantamneni E, Larhammar M, et al. Alterations in the motor neuron-rensaw cell circuit in the Sod1G93A mouse model. *J Comp Neurol* 2013;521:1449–1469.
35. Miller DJ, Bhaduri A, Sestan N, Kriegstein A. ScienceDirectShared and derived features of cellular diversity in the human cerebral cortex. *Curr Opin Neurobiol* 2019;56:117–124.
36. Thomsen GM, Gowing G, Latter J, et al. Delayed disease onset and extended survival in the SOD1G93A rat model of amyotrophic lateral sclerosis after suppression of mutant SOD1 in the motor cortex. *J Neurosci* 2014;34:15587–15600.
37. Ilieva H, Polymenidou M, Cleveland DW. Non-cell autonomous toxicity in neurodegenerative disorders: ALS and beyond. *J Cell Biol* 2009;187:761–772.
38. D'Acunzo P, Badaloni A, Ferro M, et al. A conditional transgenic reporter of presynaptic terminals reveals novel features of the mouse corticospinal tract. *Front Neuroanat* 2014;7:1–12.
39. Han Q, Cao C, Ding Y, et al. Plasticity of motor network and function in the absence of corticospinal projection. *Exp Neurol* 2015;267: 194–208.
40. Scekcic-Zahirovic J, Fischer M, Lopez GS, et al. Genetic ablation of SOD1<sup>G37R</sup> selectively from corticofugal projection neurons protects corticospinal neurons from degeneration without affecting ALS onset and progression. *bioRxiv* 2020. <https://doi.org/10.1101/2020.01.09.900944>.
41. Tremblay R, Lee S, Rudy B. GABAergic interneurons in the Neocortex: from cellular properties to circuits. *Neuron* 2016;91:260–292.
42. Gunes ZI, Kan VVY, Ye XQ, Liebscher S. Exciting complexity: the role of motor circuit elements in ALS pathophysiology. *Front Neurosci* 2020;14:573.